

## Virtual Screening of Tubercular Acetohydroxy Acid Synthase Inhibitors through Analysis of Structural Models

Dung Tien Le,<sup>†,‡</sup> Hyun-Sook Lee,<sup>†</sup> Young-Je Chung,<sup>†</sup> Moon-Young Yoon,<sup>§</sup> and Jung-Do Choi<sup>†,\*</sup>

<sup>†</sup>School of Life Sciences, Chungbuk National University, Cheongju 361-763, Korea. \*E-mail: jdchoi@chungbuk.ac.kr

<sup>‡</sup>Department of Biochemistry, University of Nebraska-Lincoln, Lincoln, NE 68588, U.S.A.

<sup>§</sup>Department of Chemistry, Hanyang University, Seoul 133-791, Korea

Received January 31, 2007

*Mycobacterium tuberculosis* is a pathogen responsible for 2-3 million deaths every year worldwide. The emergence of drug-resistant and multidrug-resistant tuberculosis has increased the need to identify new anti-tuberculosis targets. Acetohydroxy acid synthase, (AHAS, EC 2.2.1.6), an enzyme involved in branched-chain amino acid synthesis, has recently been identified as a potential anti-tuberculosis target. To assist in the search for new inhibitors and “receptor-based” design of effective inhibitors of tubercular AHAS (*Tb*AHAS), we constructed four different structural models of *Tb*AHAS and used one of the models as a target for virtual screening of potential inhibitors. The quality of each model was assessed stereochemically by PROCHECK and found to be reliable. Up to 89% of the amino acid residues in the structural models were located in the most favored regions of the Ramachandran plot, which indicates that the conformation of each residue in the models is good. In the models, residues at the herbicide-binding site were highly conserved across 39 AHAS sequences. The binding mode of *Tb*AHAS with a sulfonylurea herbicide was characterized by 32 hydrophobic interactions, the majority of which were contributed by residue Trp516. The model based on the highest resolution X-ray structure of yeast AHAS was used as the target for virtual screening of a chemical database containing 8300 molecules with a heterocyclic ring. We developed a short list of molecules that were predicted to bind with high scores to *Tb*AHAS in a conformation similar to that of sulfonylurea derivatives. Five sulfonylurea herbicides that were calculated to efficiently bind *Tb*AHAS were experimentally verified and found to inhibit enzyme activity at micromolar concentrations. The data suggest that this time-saving and cost-effective computational approach can be used to discover new *Tb*AHAS inhibitors. The list of chemicals studied in this work is supplied to facilitate independent experimental verification of the computational approach.

**Key Words :** Acetohydroxy acid synthase, *Mycobacterium tuberculosis*, Virtual screening, Swiss-Model, UCSF DOCK

### Introduction

Acetohydroxy acid synthase (AHAS) catalyzes the first step in the biosynthesis of branched-chain amino acids in plants and microorganisms. The enzyme is also a target of several known classes of herbicides, and the reaction mechanism and inhibition of plant AHAS have been studied extensively.<sup>1-4</sup> Recently, accumulating evidence suggests that AHAS could be a potential target for controlling intracellular bacteria. In 1996, Bange *et al.* showed that leucine auxotrophy restricts the growth of *Mycobacterium bovis* BCG in macrophages.<sup>5</sup> Later, inhibitors of plant AHAS were reported to also inhibit the growth of *Mycobacterium bovis* BCG *in vitro*, as well as in a mouse model.<sup>6</sup> Subsequently, *Mycobacterium avium* AHAS was cloned, expressed and characterized, and several commercial AHAS inhibitors were found to inhibit the enzyme activity at very low concentrations.<sup>7</sup> Furthermore, sulfonylureas, a class of known inhibitors of plant AHAS, were reported to inhibit the intramacrophagic multiplication of *Brucella suis*, an intracellular bacterium that causes disease in humans and animals.<sup>8</sup> In light of the increasing number of drug-resistant

bacteria, the above evidence prompts us to identify new AHAS inhibitors that could be used as anti-intracellular bacteria drugs. In our recent report using high-throughput screening of a chemical library containing more than 5000 molecules, we identified a new chemical family that inhibits *Tb*AHAS activity.<sup>9</sup> High-throughput screening of chemical libraries has proved to be a direct approach for discovering new inhibitors. Nevertheless, this method also requires the development of a high-throughput activity assay, which is often impossible for many enzymes. In addition, the method is expensive and time-consuming and sometimes produces false-positive hits due to non-specific aggregations.<sup>10</sup> The increasing number of protein structures being determined and deposited into public databases has prompted researchers to develop and employ target-based virtual screening approaches to discover new ligands (reviewed in refs.<sup>11,12</sup>). Several successes have been reported, many of which have led to the development of marketed drugs.<sup>13,14</sup> Some of the successes have highlighted the feasibility of using homology models as the target for virtual screening. For example, Schapira *et al.* successfully identified antagonists of thyroid hormone receptor by virtual screening using a computer-

modeled structure of thyroid hormone receptor.<sup>15</sup> Evers and Klebe also proved that models obtained by homology modeling are sufficient for virtual screening.<sup>16</sup>

In this work, we relied on two approaches whose validities have been thoroughly tested to identify new inhibitors of *Tb*AHAS. Deep View and Swiss Model were used for comparative modeling,<sup>17</sup> whereas UCSF DOCK was used for virtual screening.<sup>18,19</sup> The ligand database was downloaded from a well-established public chemical database developed specifically for use in virtual screening.<sup>20</sup>

## Materials and Methods

**Materials.** *M. tuberculosis* H37Rv genomic DNA was obtained from the Korean Institute of Tuberculosis (Seoul, Korea). The expression plasmid was constructed as described previously.<sup>9</sup> Herbicides were obtained from the Korean Institute of Chemical Technology (Daejeon, Korea).

**Homology modeling of *Tb*AHAS.** The AHAS sequences of *M. tuberculosis*, yeast and tobacco were aligned using BioEdit<sup>21</sup> to visualize their homology. Structural models of *Tb*AHAS were constructed as previously described for tobacco AHAS.<sup>22</sup> Briefly, the *Tb*AHAS sequence was first fitted on the yeast AHAS X-ray structures (Protein data bank IDs: 1H0N, IT9A, IT9B, IT9C); the resulting alignment was then checked and adjusted manually. The final optimized structures were then submitted for automatic modeling at the Swiss-Model server.<sup>17</sup>

**Virtual screening of *Tb*AHAS using UCSF DOCK.** The *Tb*AHAS model obtained on the highest resolution template was used to prepare the docking site. To reduce computer resource usage, only residues located within 22 Angstroms of the herbicide were selected to generate the molecular surface. The molecular surface was calculated using DMS<sup>23</sup> with the following flags [-a -n -w 1.4 -v -o]. The resulting surface was used for SPHGEN (an accessory of UCSF DOCK) to generate the outer spheres with a minimum radius of 1.4 Angstroms, not exceeding 4.0 Angstroms. The spheres were converted to PDB files for manual inspection and selection. The final spheres used for docking contain 56 spheres. The scoring grids were calculated by the accessory program GRID. The subset of molecules that contained heterocyclic rings and had a molecular weight ranging from 250-450 was created from the ZINC database (<http://zinc.docking.org>) using the search function. The molecules were downloaded and used directly for UCSF DOCK scoring. Sulfonylurea molecules were identified from the same database to ensure the same charge profile. Computation was conducted on a Pentium IV PC installed with the Linux-like CYGWIN environment ([www.cygwin.com](http://www.cygwin.com)).

Molecular visualization and visual inspection of docking results were done with UCSF Chimera,<sup>24</sup> Deep View<sup>17</sup> and Vega.<sup>25</sup>

**Determination of  $K_i$  (inhibition constant) for sulfonylurea herbicides.** The inhibition constants of several sulfonylurea inhibitors for the *Tb*AHAS catalytic subunit were determined by discontinuous assays. The reaction mixture

consisted of 100 mM potassium phosphate, pH 7.5, 1 mM ThDP, 10 mM MgCl<sub>2</sub>, 50  $\mu$ M FAD, pyruvate (2.3-25 mM), and an appropriately diluted aliquot of herbicide. The enzyme reactions were initiated by addition of catalytic subunit (0.5  $\mu$ g). The final reaction volume was 200 mL. After incubation at 37 °C for 1 hr, the reaction was terminated by the addition of sulfuric acid, and enzyme activity was determined as previously described.<sup>9</sup>

## Results

**Construction of *Tb*AHAS structures via comparative modeling.** A preliminary alignment of AHAS sequences from yeast, tobacco and *M. tuberculosis* revealed high homology (37% and 51.4% identity and similarity, respectively, data not shown). Using the approaches described previously,<sup>22</sup> four models were generated based on four different templates of yeast AHAS. The accompanying WhatCheck<sup>26</sup> reports indicated that the four models obtained of the catalytic subunits of *Tb*AHAS were of acceptable quality. As shown in Table 1, the values of RMS-Z-scores, which are close to 1.0, indicate that the four models are good.

**Evaluation of the *Tb*AHAS models.** The models' quality was initially assessed by B-factor. As shown in Figure 1, there were only a few negligibly problematic fragments; importantly, none of these fragments were located at the active site or at the herbicide-binding site. We then went further to assess the models' quality stereochemically by PROCHECK.<sup>27</sup> As shown in Figure 2 (other data not shown), the percentage of residues (except glycine and proline) located in the most favorable regions of the Ramachandran plots ranged from 87.6 to 89.0, and each model contained only 2 or 3 residues in the disallowed regions. Notably, none of these were located in the active site or in the herbicide-binding site. These results implied that the conformation of each residue in the models is realistic.

**Characterization of the herbicide-binding site and its binding mode with sulfonylureas.** As shown in Table 2 and Figure 3, the sulfonylurea-binding site of *Tb*AHAS consists of mainly hydrophobic residues and two positively charged residues (R318 and K197). These residues are highly conserved across 39 AHAS sequences. Most of the correspond-

**Table 1.** Values of the RMS Z-scores\* computed by WHATCHECK of different structural models constructed in this study

Parameters	<i>Tb</i> AHAS models based on respective yeast templates			
	1N0H	IT9A	IT9B	IT9C
Bond lengths	0.736	1.664	0.824	0.728
Bond angles	1.164	1.010	1.145	1.144
Omega angle restraints	0.949	0.914	0.902	0.764
Side chain planarity	1.659	1.118	2.004	1.588
Improper dihedral distribution	1.156	1.116	1.180	1.162
Inside/Outside distribution	1.042	1.042	1.053	1.043

\*a value close to 1.0 indicates a good model<sup>26</sup>

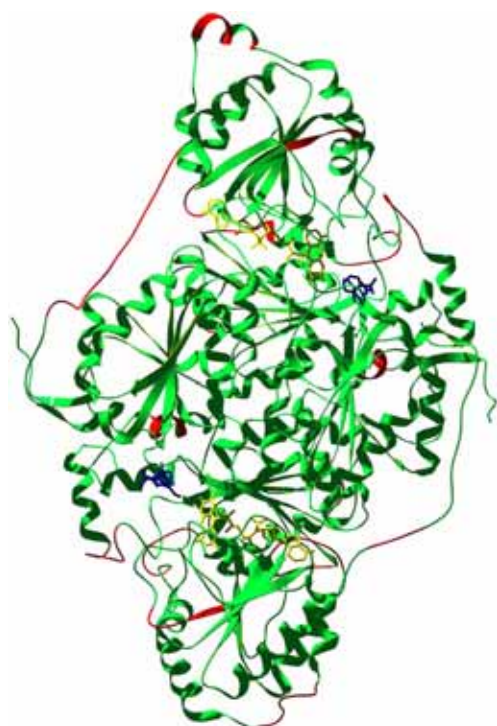


**Figure 1.** Ribbon diagram of tubercular AHAS. CS (blue) and FAD (yellow) are in stick representation. The ribbon is colored by B-factor using Deep View. The image is generated with Povray ([www.povray.org](http://www.povray.org)). Problematic fragments are red.

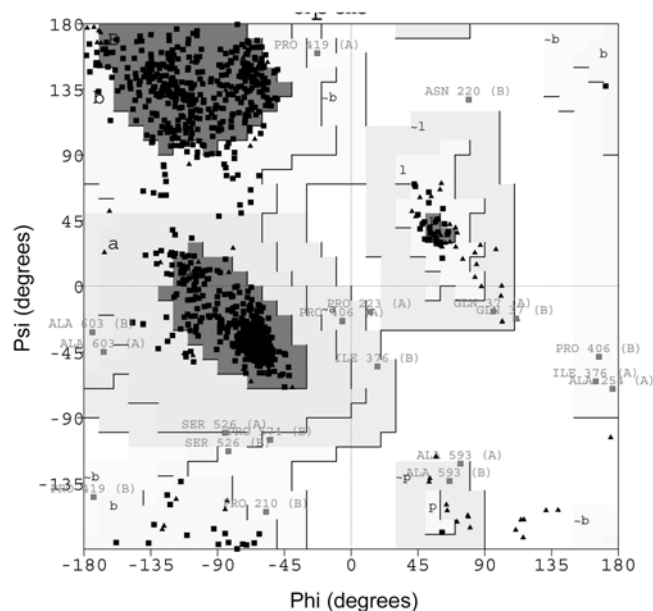


**Figure 2.** Ramachandran plot of *TbAHAS* structure built based on the highest resolution X-ray structure (1T9B). 87.8% of non-glycine and non-proline residues were located in the most favored regions, which implied that the conformation of the structural model is good. The plot was generated with web-based PROCHECK.<sup>23</sup>

ing residues in yeast and tobacco AHASs have been reported to affect herbicide sensitivity.<sup>28-36</sup> Residue L141, the second most important residue in hydrophobic interactions, was found in only 8 of out 39 sequences. However, sequences

**Table 2.** Residues located at the herbicide-binding sites of *TbAHAS* and its equivalent residues in yeast and tobacco

<i>TbAHAS</i> residues	Conserved <sup>1</sup>	Equivalent residues <sup>2</sup>	
		Yeast <sup>a</sup>	Tobacco
Gly61	39		
Gly62	35	G116	
Ala63	32	A117	A121 <sup>b</sup>
Leu65	21	L119	
Ser109	38		
Gln136	36		
Val137	39	V191	
Gly138	8	P192	
Leu141	11 <sup>3</sup>		
Ala146	35	A200	
Phe147	35		F205 <sup>c</sup>
Gln148	39		
Lys197	35	K251	K255 <sup>d</sup>
Met292	35	M354	M350 <sup>e</sup>
His293	35		H351 <sup>f</sup>
Asp317	35	D379	D375 <sup>g</sup>
Arg318	35		R376 <sup>h</sup>
Met512	37	M582	M569 <sup>e</sup>
Val513	38		V570 <sup>c</sup>
Trp516	32	W586	W573 <sup>i</sup>

<sup>1</sup>The number of sequences in which the residue is conserved among 39 AHAS sequences listed in the reference.<sup>18</sup> <sup>2</sup>Only the equivalent residues that affect herbicide sensitivity when mutated are shown. <sup>3</sup>Found only in bacteria. <sup>4</sup>As listed in reference.<sup>24</sup> <sup>5</sup>From reference.<sup>25</sup> <sup>6</sup>From reference.<sup>26</sup> <sup>7</sup>From reference.<sup>27</sup> <sup>8</sup>From reference.<sup>28</sup> <sup>9</sup>From reference.<sup>29</sup> <sup>g</sup>From reference.<sup>30</sup> <sup>h</sup>From reference.<sup>31</sup> <sup>i</sup>From reference.<sup>3</sup>

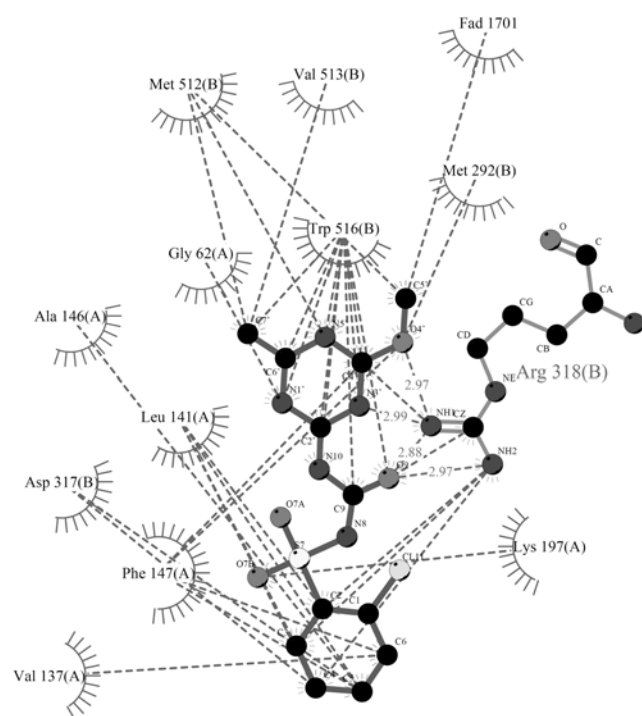


**Figure 3.** Schematic representation of the interaction between the inhibitor CS and *TbAHAS*, and the structural formula of CS. The figure was generated and analyzed using LIGPLOT.<sup>33</sup>

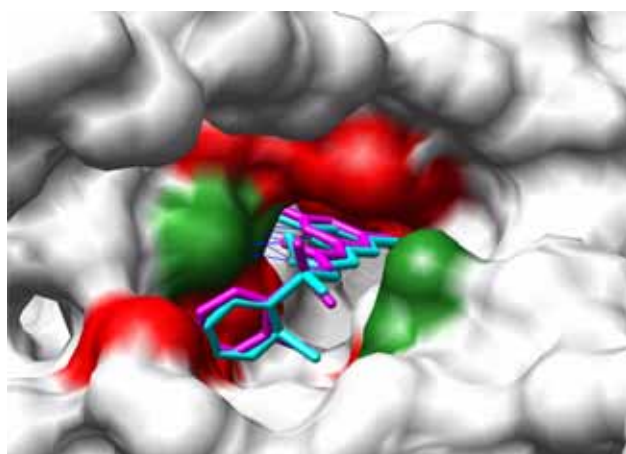


**Figure 4.** The sulfonyleurea binding site of *TbAHAS*. The substrate tunnel is occupied by the CS molecule. Protein molecule is in the surface representation. CS that was modeled by superimposition on template X-ray structure is shown in magenta stick. CS obtained by docking is shown in cyan stick. Hydrophobic residues are shown by red surface (W516, V513, M512, M292, F147, and L141). Dark green surfaces represent positively charged residues (R318, K197), and blue lines represent hydrogen bonds contributed by R318. The figure was generated using UCSF Chimera.

with this residue conserved tend to cluster together, and it was found only in AHAS sequences from bacteria, including three mycobacteria.

*TbAHAS* binds sulfonyleurea with 4 hydrogen bonds and 32 hydrophobic interactions (van der Waal interactions, *vdw*), in which the 4 hydrogen bonds are contributed by residue R318, and 16 out of 32 *vdw* interactions are due to residue W516. Residue L141 contributed 5 *vdw* interactions (Fig. 3).

#### Screening for AHAS inhibitors from a chemical subset.

In order to screen for AHAS inhibitors, we used the model built on the highest resolution template (2.2 Angstroms, IT9B) as the target. To verify the accuracy of the docking procedures and the parameter settings, we first docked the herbicide, chlorosulfuron (CS), which is also bound in the X-ray structure, on the target. As shown in Figure 4, the positions and conformations of the CS molecule calculated by UCSF DOCK and of that obtained by superimposing the model on the template were essentially the same. This result indicated that the docking procedures were highly reliable.

A subset of chemical compounds containing a hetero-

cyclic ring and having a molecular weight ranging from 250 to 450 was created from the ZINC database<sup>20</sup> (downloaded on Feb 28, 2006). The subset contained 8300 molecules. After scoring, the 400 top-ranked molecules were visualized on UCSF Chimera for conformation and binding mode with *TbAHAS*. Since binding with a ligand usually produces certain local conformational changes in a macromolecule, we proposed that only those compounds that bind to *TbAHAS* in a similar way as sulfonyleurea (bound on the target template) will have high probability to inhibit *TbAHAS* experimentally. Known and available sulfonyleurea inhibitors of AHAS were identified, downloaded from ZINC, and scored. The energy scores of the AHAS inhibitors ranged from -35 to -37 (Table 3). The inhibition constants of the five sulfonyleurea herbicides were determined, and the data showed that all five herbicides were able to inhibit enzyme activity at micromolar concentrations (Table 3). Based on the energy scores of the known AHAS inhibitors (Table 3), we decided to use an energy score cut-off value of -37.00. We then manually screened the top-ranked chemicals and obtained 137 compounds with high probability to inhibit *TbAHAS*. The top 50 compounds of the 137 chemicals identified by virtual screening are presented in Table 4.

## Discussion

Every year more than 2 million deaths are caused by *Mycobacterium tuberculosis*, a pathogen that causes tuberculosis. The emergence of drug-resistant and multidrug-resistant strains of *M. tuberculosis*<sup>39,40</sup> has put pressure on scientists to uncover alternative targets for treatment.<sup>5-7,9,41-43</sup> Among the newly discovered targets, AHAS seems to be the most promising, not only in anti-tuberculosis,<sup>5-7</sup> but also in controlling other intracellular disease-causing bacteria.<sup>8</sup> This enzyme catalyzes the common step in the biosynthesis of branched-chain amino acids in plants and microbes. It has long been the target of several structurally unrelated classes of herbicides. AHAS requires three cofactors for its catalytic function, thiamin diphosphate (ThDP), flavine adenine dinucleotide (FAD) and a divalent ion.<sup>28</sup> To further advance the search for alternative measures to control tuberculosis, we recently cloned, expressed and characterized *TbAHAS*.<sup>9</sup> The properties of the enzyme were typical of other known AHASs. For instance, *TbAHAS* was activated by the addition of regulatory subunits, and in the presence of small

**Table 3.** Inhibition constants and corresponding energy scores of known AHAS inhibitors of *TbAHAS*<sup>a</sup>

	Sulfonyleurea herbicides				
	PSE	PSM	SMM	MSM	CE
$K_{is}$ ( $\mu\text{M}$ )	$3.56 \pm 0.79$	$9.37 \pm 3.29$	$1.92 \pm 0.52$	$8.99 \pm 2.94$	$2.73 \pm 0.73$
$K_{ii}$ ( $\mu\text{M}$ )	$7.05 \pm 0.93$	$30.73 \pm 5.15$	$11.63 \pm 3.05$	$66.66 \pm 17.67$	$9.81 \pm 1.71$
Energy Scores	-35.39	-36.48	-36.50	-35.94	-37.04

<sup>a</sup>Initial rates were measured as a function of concentration of pyruvate at fixed herbicide concentration. Initial rates ( $v$ ) were fitted to noncompetitive inhibition equation [ $v = V_{\text{max}} \cdot S / \{K_m (1 + I/K_{is}) + S (1 + I/K_{ii})\}$ ] using the BASIC program designed according to the algorithms of Cleland.<sup>34</sup> In this inhibition equation, S and I are the concentrations of pyruvate and sulfonyleurea inhibitor, respectively, and  $K_{is}$  is the equilibrium constant for inhibitor dissociating from enzyme-inhibitor complex.  $K_{ii}$  is the equilibrium constant for inhibitor dissociating from the enzyme-substrate-inhibitor complex. PSE, Pyrazosulfuron ethyl; PSM, Primisulfuron methyl; SMM, Sulfometuron methyl; MSM, Metsulfuron methyl; CE, Chlorimuron ethyl.

**Table 4.** List of compounds calculated to bind *Tb*AHAS equal to or stronger than sulfonyleureas tested experimentally

No	ZINCID	Score	Chemical names
1	00420965	-44.36	ethyl 4-amino-2-(2-furylmethylcarbamoylmethylsulfanyl)pyrimidine-5-carboxylate
2	00379439	-44.34	<i>N</i> -benzyl-2-(4,6-diaminopyrimidin-2-yl)sulfanyl-acetamide
3	00351579	-44.32	2-(4,6-diaminopyrimidin-2-yl)sulfanyl- <i>N</i> -( <i>p</i> -tolyl)acetamide
4	00419238	-44.32	ethyl 4-amino-2-(tetrahydrofuran-2-ylmethylcarbamoylmethylsulfanyl)pyrimidine-5-carboxylate
5	00115798	-44.26	[4-[(4,6-diaminopyrimidin-2-yl)sulfanylmethyl]phenyl]-morpholino-methanone
6	00414325	-43.6	2-[(6-amino-9H-purin-8-yl)sulfanyl]- <i>N</i> -(3-chloro-4-methyl-phenyl)-acetamide
7	00422063	-43.44	ethyl 4-amino-2-(benzylcarbamoylmethylsulfanyl)pyrimidine-5-carboxylate
8	00422102	-43.31	ethyl 4-amino-2-( <i>p</i> -tolylcarbamoylmethylsulfanyl)pyrimidine-5-carboxylate
9	00420141	-43.17	2-(4,6-diaminopyrimidin-2-yl)sulfanyl- <i>N</i> -(tetrahydrofuran-2-ylmethyl)acetamide
10	00085259	-42.93	<i>N</i> -[(4,6-dimethylpyrimidin-2-yl)amino-(3-methoxyphenyl)amino-methylene]propanamide
11	00415632	-42.87	<i>N</i> -[4-[2-(4,6-diaminopyrimidin-2-yl)sulfanylacetyl]phenyl]propanamide
12	00308194	-42.36	2-[4-(2-methylprop-2-enyl)piperazin-1-yl]-7-phenyl-3,5,7,8-tetraza-bicyclo[4.3.0]nona-2,4,8,10-tetraene
13	00379439	-41.7	<i>N</i> -benzyl-2-(4,6-diaminopyrimidin-2-yl)sulfanyl-acetamide
14	00285367	-41.5	2-(1,3-dimethyl-2,6-dioxo-purin-7-yl)- <i>N</i> -(4,6-dimethylpyrimidin-2-yl)-acetamide
15	04596862	-41.56	5-[(4-isobutoxyphenyl)methyl]-2-methylsulfanyl-pyrimidine-4,6-diol
16	00417147	-41.4	4-(4,6-diaminopyrimidin-2-yl)sulfanyl-3-oxo- <i>N</i> -phenyl-butanamide
17	03878082	-41.39	5-[(4-isobutoxyphenyl)methyl]-2-sulfanyl-pyrimidine-4,6-diol
18	00202125	-41.38	2-(1H-benzoimidazol-2-ylsulfanyl)- <i>N</i> -(4,6-dimethoxypyrimidin-2-yl)-acetamide
19	00417745	-41.3	ethyl 4-amino-2-[2-(3-methoxyphenyl)-2-oxo-ethyl]sulfanyl-pyrimidine-5-carboxylate
20	00092402	-41.29	2-[(3-phenyl-1,2,4-oxadiazol-5-yl)methylsulfanyl]pyrimidine-4,6-diamine
21	00419913	-41.26	2-(4,6-diaminopyrimidin-2-yl)sulfanyl- <i>N</i> -(4-dimethylaminophenyl)-acetamide
22	00023472	-41.24	4-amino- <i>N</i> -[2,6-bis(methylamino)pyrimidin-4-yl]-benzenesulfonamide
23	00420699	-41.14	2-(4,6-diaminopyrimidin-2-yl)sulfanyl- <i>N</i> -(4-methoxyphenyl)-propanamide
24	00250336	-41.05	<i>N</i> -phenyl- <i>N'</i> -(tetrahydrofuran-2-ylmethyl)quinazoline-2,4-diamine
25	00412982	-40.97	2-(4,6-diaminopyrimidin-2-yl)sulfanyl-1-(4-ethylpiperazin-1-yl)-ethanone
26	00420699	-40.95	2-(4,6-diaminopyrimidin-2-yl)sulfanyl- <i>N</i> -(4-methoxyphenyl)-propanamide
27	00392447	-40.93	4-amino- <i>N</i> -(5-ethoxypyrimidin-2-yl)-benzenesulfonamide
28	00172593	-40.86	3-benzyl-8-benzylsulfanyl-purin-6-amine
29	00419945	-40.85	2-(4-amino-5-cyano-pyrimidin-2-yl)sulfanyl- <i>N</i> -(2,4-dimethoxyphenyl)-acetamide
30	00421019	-40.6	2-(4,6-diaminopyrimidin-2-yl)sulfanyl- <i>N</i> -(3,4-dimethylphenyl)-acetamide
31	00269132	-40.6	2-[(4-methoxyphenyl)methyl]- <i>N</i> -(tetrahydrofuran-2-ylmethyl)quinazolin-4-amine
32	00419243	-40.55	ethyl 4-amino-2-[2-oxo-2-( <i>p</i> -tolyl)ethyl]sulfanyl-pyrimidine-5-carboxylate
33	00269135	-40.45	2-[(4-methoxyphenyl)methyl]- <i>N</i> -(tetrahydrofuran-2-ylmethyl)quinazolin-4-amine
34	00390789	-40.4	4-amino- <i>N</i> -[4-(2-furyl)-6-methyl-pyrimidin-2-yl]-benzenesulfonamide
35	00426478	-40.39	<i>N,N</i> -diethyl- <i>N'</i> -[7-( <i>m</i> -tolyl)-3,5,7,8-tetraza-bicyclo[4.3.0]nona-2,4,8,10-tetraen-2-yl]-ethane-1,2-diamine
36	00421734	-40.33	<i>N</i> -(4-acetylphenyl)-2-(4-amino-5-cyano-pyrimidin-2-yl)sulfanyl-acetamide
37	00445298	-40.31	1-(4,6-dimethylpyrimidin-2-yl)-3-(4-sulfamoylphenyl)-guanidine
38	00422367	-40.3	<i>N</i> -(4-acetylphenyl)-2-(4,6-diaminopyrimidin-2-yl)sulfanyl-propanamide
39	00422102	-40.29	ethyl 4-amino-2-( <i>p</i> -tolylcarbamoylmethylsulfanyl)pyrimidine-5-carboxylate
40	00269215	-40.23	1-(2,4-dimethylphenyl)-3-(4-methyl-6-morpholino-pyrimidin-2-yl)-guanidine
41	00102430	-40.16	1-(4,6-dimethylpyrimidin-2-yl)-3-(2-naphthyl)guanidine
42	00382378	-40.15	2-(4,6-diaminopyrimidin-2-yl)sulfanyl- <i>N</i> -(5-fluoro-2-methyl-phenyl)-acetamide
43	00420138	-40.06	2-(4,6-diaminopyrimidin-2-yl)sulfanyl-1-(2-methylindolin-1-yl)-ethanone
44	00419237	-40.02	ethyl 4-amino-2-(tetrahydrofuran-2-ylmethylcarbamoylmethylsulfanyl)pyrimidine-5-carboxylate
45	00385035	-40.01	<i>N,N'</i> -bis(4-methoxyphenyl)pyrimidine-2,4-diamine
46	00049139	-39.98	4-amino- <i>N</i> -(2,6-dimethoxypyrimidin-4-yl)-benzenesulfonamide
47	00085261	-39.96	<i>N</i> -[(4,6-dimethylpyrimidin-2-yl)amino-(3-methoxyphenyl)amino-methylene]propanamide
48	00034128	-39.91	2-[(6-amino-9H-purin-8-yl)sulfanyl]- <i>N</i> -( <i>p</i> -tolyl)acetamide
49	00414321	-39.87	2-[(6-amino-9H-purin-8-yl)sulfanyl]- <i>N</i> -(3,5-dimethylphenyl)-acetamide
50	00250328	-39.86	3-[4-(2-furylmethylamino)quinazolin-2-yl]aminophenol

subunits, it was inhibited by branched-chained amino acids. Notably, its activity was also inhibited by several known AHAS inhibitors.<sup>9</sup>

In this investigation, we first generated structural models of *Tb*AHAS and then analyzed the binding mode with a sulfonyleurea herbicide. As shown in Figure 3, the interaction

between *Tb*AHAS and its inhibitor was stabilized mostly by *vdw* contacts. The majority of these *vdw* contacts were established between residue W516 of *Tb*AHAS and the heterocyclic ring of the inhibitor (Fig. 3, 4). Since the heterocyclic ring contributed exclusively to the *vdw* contacts, we assumed that the interaction of this particular region of the

inhibitor with *Tb*AHAS is at its strongest potential. Therefore, altering this part of the inhibitor may not improve binding. Thus, we searched for and downloaded all compounds that contain a heterocyclic ring and whose molecular weight ranged from 250–450 in the ZINC database<sup>20</sup> to use in virtual screening against the *Tb*AHAS inhibitor-binding site. This search and download resulted in a database containing 8300 compounds. The target site was prepared as suggested in the UCSF DOCK manuals, which are freely available at the program's homepage (<http://dock.compbio.ucsf.edu/>), and UCSF DOCK 5.6.0 was used for database scoring. Known AHAS inhibitors were also identified, downloaded from ZINC, and scored in a separate batch. The energy scores of AHAS inhibitors that inhibited *Tb*AHAS experimentally at micromolar concentrations ranged from –35 to –37 (Table 3); hence, we used –37 as the cut-off value to identify the top-ranked compounds. All compounds with energy score equal or greater (more negative) than –37 underwent visual inspection. During visual inspection, compounds whose conformations and binding mode with *Tb*AHAS differed significantly from that of sulfonylureas were further excluded. After all of these steps, we compiled a list of 137 chemicals, the top 50 of which are listed in Table 4. The top 50 compounds listed, which have energy score greater (more negative) than –39, are expected to be stronger *Tb*AHAS inhibitors than five sulfonylurea herbicides tested experimentally in this study.

The computational approaches employed in this study have proved to be reliable,<sup>11–20,22,44</sup> while the short list of compounds from our study provides an opportunity for independent experimental testing. Our detailed analysis of the binding mode of *Tb*AHAS with sulfonylureas also provides fundamental information for the structure-based design of effective inhibitors against *Tb*AHAS.

**Acknowledgement.** This work was supported by the Korea Research Foundation Grant funded by the Korean Government (MOEHRD) (The Regional Research Universities Program/Chungbuk BIT Research-Oriented University Consortium).

## References

- Hwang, J. H.; Kim, J. M.; Kim, Y. T.; Choi, J. D.; Yoon, M. Y. *Bull. Korean Chem. Soc.* **2003**, *24*, 1856.
- Kim, J. M.; Kim, J. R.; Kim, Y. T.; Choi, J. D.; Yoon, M. Y. *Bull. Korean Chem. Soc.* **2004**, *25*, 721.
- Le, D. T.; Choi, J. D. *Bull. Korean Chem. Soc.* **2005**, *26*, 916.
- Karim, M.; Shim, M. Y.; Kim, J. M.; Choi, K. J.; Kim, J. R.; Choi, J. D.; Yoon, M. Y. *Bull. Korean Chem. Soc.* **2006**, *27*, 549.
- Bange, F. C.; Brown, A. M.; Jacobs, W. R. Jr. *Infect. Immun.* **1996**, *64*, 1794.
- Grandoni, J. A.; Marta, P. T.; Schloss, J. V. *J. Antimicrob. Chemother.* **1998**, *42*, 475.
- Zohar, Y.; Einav, M.; Chipman, D. M.; Barak, Z. *Biochim. Biophys. Acta* **2003**, *1649*, 97.
- Boige grain, R. A.; Liautard, J. P.; Kohler, S. *Antimicrob Agents Chemother.* **2005**, *49*, 3922.
- Choi, K. J.; Yu, Y. G.; Hahn, H. G.; Choi, J. D.; Yoon, M. Y. *FEBS Lett.* **2005**, *579*, 4903.
- McGovern, S. L.; Caselli, E.; Grigorieff, N.; Shoichet, B. K. *J. Med. Chem.* **2002**, *45*, 1712.
- Shoichet, B. K. *Nature* **2004**, *432*, 862.
- Shoichet, B. K.; McGovern, S. L.; Wei, B.; Irwin, J. J. *Curr. Opin. Chem. Biol.* **2002**, *6*, 439.
- Itzstein, M. von; Wu, W.-Y.; Kok, G. B.; Pegg, M. S.; Dyason, J. C.; Jin, B.; Phan, T. V.; Smythe, M. L.; White, H. F.; Oliver, S. W.; Colman, P. M.; Varghese, J. N.; Ryan, D. M.; Woods, J. M.; Bethell, R. C.; Hotham, V. J.; Cameron, J. M.; Penn, C. R. *Nature* **1993**, *363*, 418.
- Varney, M. D.; Marzoni, G. P.; Palmer, C. L.; Deal, J. G.; Welsh, S. K. M.; Bacquet, R. J.; Bartlett, C. A.; Morse, C. A.; Booth, C. L. J.; Herrmann, S. M.; Howland, E. F.; Ward, R. W.; White, J. J. *Med. Chem.* **1992**, *35*, 663.
- Schapiro, M.; Raaka, B. M.; Das, S.; Fan, L.; Totrov, M.; Zhou, Z.; Wilson, S. R.; Abagyan, R.; Samuels, H. H. *Proc. Natl. Acad. Sci. U.S.A.* **2003**, *100*, 7354.
- Evers, A.; Klebe, G. *Angew. Chem. Int. Ed.* **2004**, *43*, 248.
- Schwede, T.; Kopp, J.; Guex, N.; Peitsch, M. C. *Nucleic Acids Res.* **2003**, *31*, 3381.
- Shoichet, B.; Bodian, D. L.; Kuntz, I. D. *J. Comput. Chem.* **1992**, *13*, 380.
- Lorber, D. M.; Udo, M. K.; Shoichet, B. K. *Protein Sci.* **2002**, *11*, 1393.
- Irwin, J. J.; Shoichet, B. K. *J. Chem. Inf. Model.* **2005**, *45*, 177.
- Hall, T. A. *Nucleic Acids Symp. Ser.* **1999**, *41*, 95.
- Le, D. T.; Yoon, M.-Y.; Kim, Y. T.; Choi, J.-D. *Biophys. Res. Commun.* **2004**, *317*, 930.
- Richards, F. *Annu. Rev. Biophys. Bioeng.* **1977**, *6*, 151.
- Pettersen, E. F.; Goddard, T. D.; Huang, C. C.; Couch, G. S.; Greenblatt, D. M.; Meng, E. C.; Ferrin, T. E. *J. Comput. Chem.* **2004**, *25*, 1605.
- Pedretti, A.; Villa, L.; Vistoli, G. *J. Comp. Aid. Mol. Des.* **2004**, *18*, 167.
- Vriend, G. *J. Mol. Graph.* **1990**, *8*, 52.
- Laskowski, R. A.; MacArthur, M. W.; Moss, D. S.; Thornton, J. M. *J. Appl. Cryst.* **1993**, *26*, 283.
- Duggleby, R. G.; Pang, S. S. *J. Biochem. Mol. Biol.* **2000**, *33*, 1.
- Chong, C. K.; Choi, J. D. *Biochem. Biophys. Res. Commun.* **2000**, *279*, 462.
- Jung, S.-M.; Le, D. T.; Yoon, S.-S.; Yoon, M.-Y.; Kim, Y. T.; Choi, J.-D. *Biochem. J.* **2004**, *383*, 53.
- Yoon, T. Y.; Chung, S. M.; Chang, S. I.; Yoon, M. Y.; Hahn, T. R.; Choi, J. D. *Biochem. Biophys. Res. Commun.* **2002**, *293*, 433.
- Le, D. T.; Yoon, M.-Y.; Kim, Y. T.; Choi, J.-D. *Biochem. Biophys. Res. Commun.* **2003**, *306*, 1075.
- Oh, K. J.; Park, E. J.; Yoon, M. Y.; Han, T. R.; Choi, J. D. *Biochem. Biophys. Res. Commun.* **2001**, *282*, 1237.
- Le, D. T.; Yoon, M.-Y.; Kim, Y. T.; Choi, J.-D. *BBA-Proteins and Proteomics* **2005**, *1749*, 103.
- Le, D. T.; Yoon, M. Y.; Kim, Y. T.; Choi, J. D. *J. Biochemistry (Tokyo)* **2005**, *138*, 35.
- Chong, C. K.; Shin, H. J.; Chang, S. I.; Choi, J. D. *Biochem. Biophys. Res. Commun.* **1999**, *259*, 136.
- Wallace, A. C.; Laskowski, R. A.; Thornton, J. M. *Prot. Eng.* **1995**, *8*, 127.
- Cleland, W. W. *Methods Enzymol.* **1979**, *63*, 103.
- Frieden, T. R.; Sterling, T. R.; Munsiff, S. S.; Watt, C. J.; Dye, C. *Lancet.* **2003**, *362*, 887.
- Barnes, P. F.; Cave, M. D. *N. Engl. J. Med.* **2003**, *349*, 1149.
- Xu, S.; Yang, Y.; Jin, R.; Zhang, M.; Wang, H. *Protein Expr. Purif.* **2006**, in press.
- Maxwell, A. *Trends Microbiol.* **1997**, *5*, 102.
- Fonseca, I. O.; Magalhaes, M. L.; Oliveira, J. S.; Silva, R. G.; Mendes, M. A.; Palma, M. S.; Santos, D. S.; Basso, L. A. *Protein Expr. Purif.* **2006**, *46*, 429.
- Irwin, J. J.; Raushel, F. M.; Shoichet, B. K. *Biochemistry* **2005**, *44*, 12316.